Key Engineering Materials
ISSN: 1662-9795, Vol. 926, pp 426-435
doi:10.4028/p-fu152h

Submitted: 2021-12-08
Revised: 2022-01-26
Accepted: 2022-01-28
Online: 2022-07-22

Simulation of Coarse Grain Evolution During Hot Extrusion of Al-Mg-Si Alloys

J. Kronsteiner[1, a* *], S. Hovden[1, b], A. Arnoldt[1, c], and J. A. Österreicher[1, d]

LKR Light Metals Technologies, Austrian Institute of Technology, Giefinggasse 2, 1210 Vienna, Austria

[a]johannes.kronsteiner@ait.ac.at, [b]sindre.hovden@ait.ac.at, [c]aurel.arnoldt@ait.ac.at, [d]johannes.oesterreicher@ait.ac.at

Keywords: Microstructure Modelling, Metal Extrusion, FEM, Geometric Dynamic Recrystallization

Abstract. Coarse grains at or near the surfaces of extruded aluminum profiles can have a major detrimental influence on their ductility and surface quality. Thus, the extrusion industry aims to minimize coarse grains while increasing the productivity of the process. Peripheral Coarse Grains (PCG) develop depending on local state variables such as temperature, strain and strain rate. Here we present a microstructure based material model implemented into HyperXtrude™, capable of predicting the development of PCG by combining geometric Dynamic Recrystallization (gDRX) and conventional grain growth models. Due to its history dependence, the model is implemented to run during the whole transient extrusion simulation. The first results of the predicted ram force as well as final grain distribution in the profile show reasonable agreement with experimental trials and electron backscattered diffraction results.

Introduction

The aim in the metal extrusion industry is to increase the productivity of the process while maintaining or improving the product quality. The mechanical properties are strongly influenced by grain size, among other factors. Grain size is influenced, for instance, by localized recrystallization (e.g. around the periphery, hence known as Peripheral Coarse Grain, PCG) [1]. The ductility, surface quality, fatigue and corrosion properties of extruded products, however, can considerably deteriorate due to coarse grains at or near the surfaces of extruded profiles. Coarse grains develop depending on local state variables such as temperature, strain and strain rate [2]. The influence of those state variables on the PCG formation of 6xxx-series aluminium alloys was investigated by [3]. They found that for a given chemical composition, the microstructure of extruded profiles could be significantly altered by carefully controlling the process parameters. Since grain growth is promoted by high temperature and high strains, there is a potential conflict between maintaining small grain sizes and aiming to increase the efficiency of the process by increasing temperature and ram speeds. However, Sweet et al. [3] proposed some possible strategies: One can either prevent the formation of PCG or one can promote recrystallization and aim for a fully recrystallized microstructure. Grain growth after the die exit is also influenced by cooling capabilities. Different approaches may be suitable for different alloys: Depending on alloy compositions, grain growth can happen between the die exit and any cooling process at the lead-out table [4]. If recrystallization during this time happens, it is called static recrystallization. However, for optimization that does not rely on trial-and-error, knowledge about microstructure evolution based on the chemical composition and combination of process parameters is necessary. Since the microstructure in complex extrusion profiles is locally very different, the geometry needs to be considered as well. In current publications concerning extrusion simulations including microstructure, mainly simple geometries or even only 2D simulations are considered. The implementation of the developed physically-based microstructure model into HyperXtrude™ ensures that industrially relevant geometries and process parameters can be used. The prediction and the controlling of grain growth are therefore essential parts for further improvements of the product quality.

Method

According to [2], the formation of Peripheral Coarse Grain (PCG) can be explained by conventional nucleation and growth theories. Additionally, Dynamic Recrystallization (DRX, [5]) was found to affect PCG formation to a certain extent [6]. DRX can be subdivided again, where continuous Dynamic Recrystallization (cDRX) and geometric Dynamic Recrystallization (gDRX) may occur during hot extrusion of aluminum [2]. The formation of coarse grain was explained by [2] for 7xxx aluminium alloys as static recrystallization (SRX) of partially recrystallized grains. These partially recrystallized grains mainly develop by geometric Dynamic Recrystallization (gDRX) according to [7]. Geometric DRX takes place when the thickness of the deforming grains (initial grain size, d_0) equals the subgrain size (δ) [7]. In Figure 1, the mechanism of gDRX is schematically depicted. The assumption is that due to large strains caused by severe deformation, the deformed grain thickness can approach the subgrain size. As depicted in Figure 1 (a) to (c), High Angle Grain Boundaries (HAGB) become squeezed together until they contact each other. If that is the case, defragmentation of grains can occur (see Figure 1, (d) - (e)) to form fine recrystallized grains. According to [7], cDRX has only minor to no effect dur-

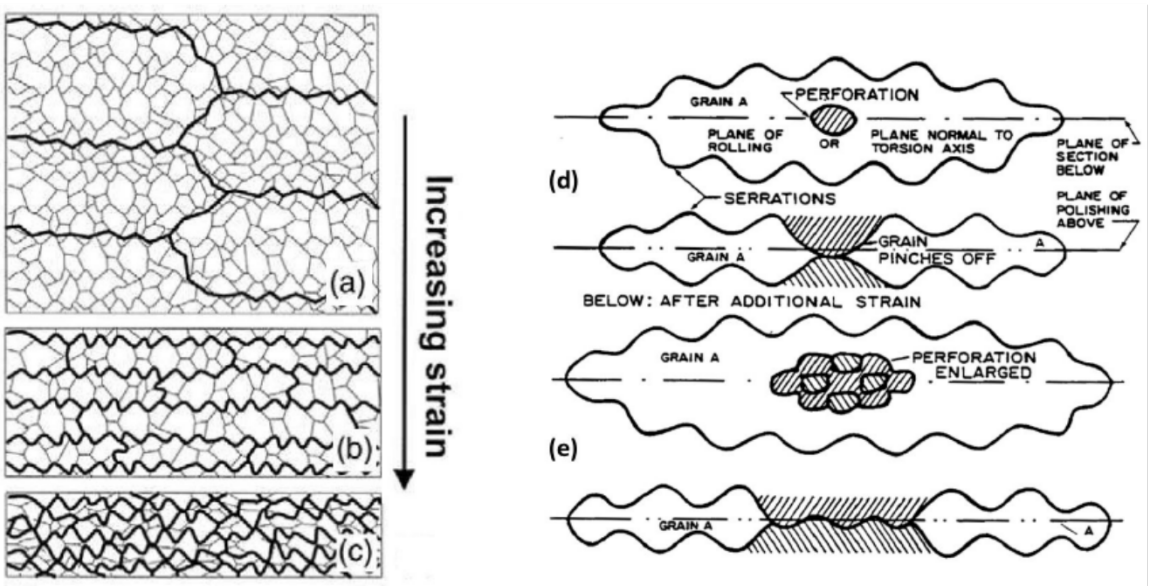

Fig. 1: Schematic representation of mechanisms leading to gDRX. An increase in strain can lead to a decrease of distance between high grain angle boundaries (HAGB - bold lines) while subgrains (lighter lines) stay approximately unchanged ((a) - (c), [8]). At some point, HAGB contact each other and lead to a separation of large elongated grains into smaller grains ((d) - (e), [9]).

ing hot extrusion of aluminum. Therefore, only gDRX is considered in the presented implementation of the model from [7] in HyperXtrude™. In contrast to the already published investigations of [2], the presented model was directly implemented into the material UDF of HyperXtrude™ which means that the calculations are performed for every element and each time step of the mesh. This is similar to the implementation of [7] were only 2D was considered, however. In this paper, first results of 3D simulations of medium complex extrusion geometries are presented for AA6082 aluminum alloy. The implementation in HyperXtrude™ allows to further increase the geometric complexity in future.

Simulation Framework

The implemented Mean Dislocation Density Material (MD²M) model consists of a flow stress and a grain morphology part and is based on [7].

Flow stress model

The calculation of the flow stress is based on the Kocks-Mecking approach [10, 11]. Here, the evolution of microstructure during thermo-mechanical processing is described in terms of the evolution of

dislocation density (ρ). Hardening as well as recovery are modelled as production of dislocations and their annihilation, respectively. The evolution of mean dislocation density ρ from time step $t-1$ to t is described by

$$\frac{\mathrm{d}\rho^t}{\mathrm{d}t} = \frac{M \cdot \dot{\varphi}}{b}\left(\frac{\sqrt{\rho^{t-1}}}{A} - B \cdot d_{ann} \cdot \rho^{t-1}\right) - C \cdot D_s \frac{G\left(T\right) \cdot b^3}{k_b \cdot T}\left[\left(\rho^{t-1}\right)^2 - \left(\rho_{eq}\right)^2\right]. \quad (1)$$

The first term on the right-hand side of Equation 1 describes the work hardening due to the increase in dislocation density. The second term describes the softening due to spontaneous annihilation and the third term describes the thermally activated dislocations climb.
The flow stress is calculated by starting from the initial yield stress σ_y (first term on the right-hand side of Equation 2). The work hardening based on the evolution of dislocation density (second term) as well as the subgrain boundary hardening (third term) give the final flow stress as

$$\sigma^t = \sigma_y + M \cdot G\left(T\right) \cdot b \cdot \sqrt{\rho^t} \cdot \left[0.5 + \left(\frac{1}{K}\right)\right]. \quad (2)$$

The subgrain boundary energy γ_{sub}, which is only used by the static recrystallization model, is calculated inside of the flow stress model based on the accumulated dislocation density ρ_g and used in Equation 9 by

$$\gamma_{sub}^t = \gamma_{sub}^{t-1} + \frac{C1}{\sqrt{\rho_g^t}} \cdot G\left(T\right) \cdot b^2 \cdot C2 \cdot \mathrm{d}\rho_g^t. \quad (3)$$

The variables used in Eqs. 1-3 are summarized in Table 1.

Table 1: Parameters and constants of Eqs.(1) - (3)

Description	Variable		
Taylor factor for random (fcc) textures	M	3.06	[-]
Length of the Burgers vector	b	28.6	$[nm]$
Alloy specific fitting parameters	$A, B, C, K, C1, C2$		
Local strain rate	$\dot{\varphi}$	calculated	
Critical distance for spontaneous annihilation	d_{ann}	calculated	
Diffusion coefficient in solid state	D_s	calculated	
Temperature dependent shear modulus	$G\left(T\right)$	calculated	
Temperature	T	calculated	
Boltzmann constant	k_b	1.381e-23	$[J/K]$
Dislocation density (equilibrium)	ρ, ρ_{eq}	1.0e+11	$[m^{-2}]$
Retarding force (Zener drag) [12, 13]	$P_{Z,sub}$	calculated	
Subgrain size (equilibrium)	ρ, δ_{eq}	calculated	
Accumulated dislocation density without recovery	ρ_g^t	calculated	
Flow stress at current time step	σ^t	calculated	

To consider the alloy specific forming behavior, three fitting parameters A, B and C [14], are used. The temperature and strain rate dependent parameters A, B and C were determined by fitting the simulated flow stress results to the experimentally determined results for several strain rates and temperatures.

Static recrystallization model

The static recrystallization model implemented into the User Defined Material (UDF) subroutine of HyperXtrude™ calculates grain growth and static recrystallization during heat treatment processes. Depending on the state of recrystallization, grain diameter d^t at time t is either calculated by

$$d^t = d^{t-1} + M \cdot \left(\frac{3 \cdot \gamma_{gb}}{d^{t-1}} + P_D - P_Z\right) \cdot dt, \quad (4)$$

or during recrystallization ($X^{t-1} > 0$) by

$$d^t = d^{t-1} \cdot \left(1 - X^{t-1}\right) + d_{rex}^{t-1} \cdot X^{t-1}. \tag{5}$$

Grain diameter d^t during static recrystallization (in Equation 5) depends on the current grain diameter d^{t-1} as well as the recrystallized grain diameter d_{rex}^{t-1} and the recrystallized fraction X^{t-1}. This means that the calculated average grain diameter d^t represents a mixture of original (d^{t-1}) and recrystallized (d_{rex}^{t-1}) grains. The recrystallized grain diameter d_{rex}^t at time t is calculated by

$$d_{rex}^t = d_{rex}^{t-1} + M \cdot \left(P_D^{t-1} - P_Z\right) \cdot \left(1 - X^{t-1}\right) \cdot dt. \tag{6}$$

The recrystallized grain fraction X^t at time t is calculated by

$$X^t = X^{t-1} + \frac{\pi}{6}\left[\Delta N \cdot \left(d_{rex}^{t-1}\right)^3 + N^{t-1} \cdot 3 \cdot \left(d_{rex}^{t-1}\right)^2 \cdot \frac{\mathrm{d}d_{rex}^t}{\mathrm{d}t}\right]. \tag{7}$$

Peripheral Coarse Grain (PCG) develops in geometrically recrystallized areas through continuous grain growth [2]. The GDRX indicator is calculated by the flow stress model according to

$$X_{gDRX} = \begin{cases} 1 & \text{if } \delta^t \geq d_0 \exp(-\varphi^t) \\ 0 & \text{if } \delta^t < d_0 \exp(-\varphi^t) \end{cases} \tag{8}$$

X_{gDRX} depends on the current plastic strain φ^t and on whether the deformed initial grain size d_0 approaches the subgrain diameter δ^t (see Figure 1). The subgrain diameter (δ^t) at time t in Equation 8 is calculated by

$$\delta^t = \delta^{t-1} + 3 \cdot M \cdot \gamma_{sub}\left(\frac{1}{\delta^{t-1}} - \frac{1}{\delta_{eq}} - P_{Z,sub}\right) \cdot dt. \tag{9}$$

In dynamically recrystallized areas, d^t can grow without obstruction by static recrystallization until the grain size approaches $3 \cdot \gamma_{gb}$ (see Equation 4).
The parameters in Eqs. (4) - (8) are summarized in Table 2.

Table 2: Parameters and constants of (4) - (8).

Description	Parameter
Strain	φ
Grain diameter	d
Grain diameter	d_0
Recrystallized grain diameter	d_{rex}
Grain boundary energy	γ_{gb}
Recrystallized grain fraction	X
Driving force (stored energy)	P_D
Retarding force (Zener Drag)	$P_Z, P_{Z,sub}$
Number of nucleii	N
Change in number of nucleii	ΔN

Experimental Procedure

Light Metals Technologies Ranshofen (LKR) owns a semi-industrial extrusion press (type Müller Engineering NEHP 1500.01), used to perform the experiments. To promote PCG, a so called ”ruler” profile was produced. Due to its significance for the metal extrusion industry, AA6082 was chosen for all the investigations. Extrusion billets of 65 mm diameter and 230 mm length were cast by gravity

die casting at LKR and subsequently homogenized at 540 °C for 4 h. The composition of the alloy was measured using a Spectro Spectromaxx 6 optical emission spectrometer (SPECTRO Analytical Instruments GmbH, Kleve, Germany) and is given in Table 3.

Table 3: Alloy composition in wt.-% used for investigations.

Alloy	Al	Si	Fe	Cu	Mn	Mg	Cr
AA6082	97.0	1.02	0.19	0.11	0.67	0.89	0.16

Light microscopy (LM) was used to get an overview of the structure. In order to make the grain structure more visible, the sections were electrolytically etched according to Barker and viewed using polarisation filters. Furthermore backscattered electron (BSE) microscopy and electron backscattered diffraction (EBSD) of the extrusion profiles were performed using a TESCAN Mira 3 scanning electron microscope at 20 kV accelerating voltage and a working distance of 10 and 20 mm, respectively. For the EBSD measurements, a Hikari Plus EBSD camera from EDAX was used. A total of 7 maps with a view field of approx. 1500 µm each and a step size of 8 µm were taken and stitched together (covering almost half of the profile). The data were analyzed with the software OIM Analysis (version 8.5), applying a clean up for Grain Dilation and Neighbour CI Correlation (one iteration).

The volume fraction and mean diameter of nanoscale particles (dispersoids) is necessary for the calculation of the Zener Drag (P_Z, $P_{Z,sub}$) in the recrystallization part of the MD²M model. The areal size distribution of dispersoids was obtained by measuring the equivalent circular diameter of several hundred dispersoids in BSE micrographs. To obtain a volume fraction and a mean diameter corrected for information depth, the areal size distribution was converted into a volumic one using the stereological method of [15], which is based on Monte-Carlo simulation of BSE information depth for different dispersoid diameters. The results are shown in Figure 2.

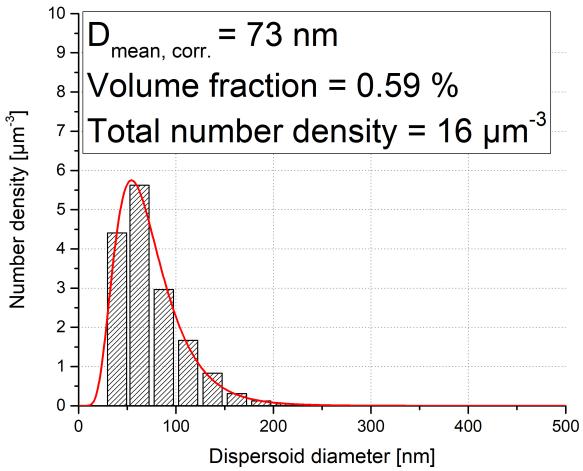

Fig. 2: Histogram of dispersoid number density per volume for the homogenized sample. The dispersoids were counted in the extruded state.

To tailor the material model to the investigated alloy, the alloy specific fitting parameters needed to be found (see Table 1). Compression tests of the homogenized samples were performed for different temperatures (450, 480 and 510 °C) and strain rates (0.1, 1.0 and 10.0 s^{-1}) using Bähr DIL805 A/D dilatometer (TA Instruments, USA). The raw data from the dilatometer was evaluated and improved using the LKR flow stress analysis tool.

Numerical Model

All simulation results shown in this paper were obtained using the user-defined material model MD²M (see section Simulation framework) implemented into Altair HyperXtrude™ 2021.1. The flow stress part was mainly used for the metal extrusion process, the recrystallization/grain growth part was active during the ”heat treatment” phase. The so-called heat treatment phase is the assumed transfer of the finished profile from the exit of the die to the cooling facilities. This transfer time is simply simulated by keeping the temperature constant and thus giving the recrystallization model time for the growth of the grains.
At the start of the hot metal extrusion process, a pre-heated cast billet was inserted into the extrusion press. The considered ”ruler” profile was then extruded by pushing the hot material through a shape-giving die. The FEM model showing the mesh (Figure 3a) and the dimensions of the profile (Figure 3b) are given below. The billet consisted of rather coarse mainly equi-axed and quite uniformly distributed

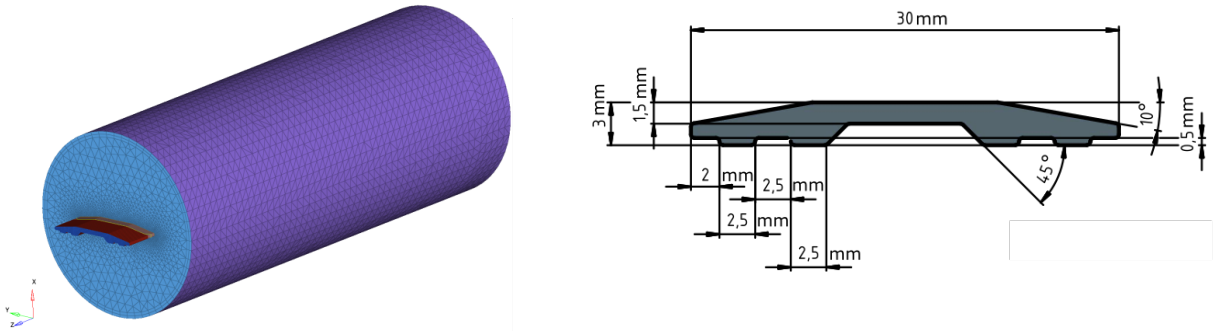

(a) (b)

Fig. 3: FEM extrusion model (a) and CAD model of the extrusion profile (b).

grains. One of the input parameters for the grain growth model was therefore the average grain size of the cast billet. This and other important material parameters are given in Table 4.

Table 4: Relevant material parameters

Density $[kgm^{-3}]$	2680
Young’s Modulus $[Nm^{-2}]$	4.6e+10
Poisson Ratio $[m^{-3}]$	0.36
Initial grain size $[\mu m]$	250
Number density of dispersoids $[\mu m^{-3}]$	16
Diameter of dispersoids $[nm]$	73
Specific Heat $[Jkg^{-1}K^{-1}]$	1017
Conductivity $[Wm^{-1}K^{-1}]]$	217
Reference Temperature $[K]$	773
Liquidus Temperature $[K]$	916
Solidus Temperature $[K]$	877

The process parameters for the numerical model were set to be consistent with the extrusion experiment, and can be found in Table 5. The boundary conditions can be found in the same table.

Table 5: Process parameters and boundary conditions

Initial container temperature $[°C]$	484
Initial die temperature $[°C]$	490
Initial billet temperature $[°C]$	478
Ram speed $[mms^{-1}]$	1.0
Extrusion ratio	1:48
HTC billet-die $[Wm^{-2}K^{-1}]$	1000
HTC billet-container $[Wm^{-2}K^{-1}]$	1000

For all contact conditions, the sticking friction model was used. A script for changing the ram speed allowed to reproduce the ram speed of the experiment and to set the ram speed to zero after half of the billet was extruded. This was used as a trigger to change from the flow stress model to the static recrystallization (grain growth) model. Finally, computational parameters are summarized in Table 6.

Table 6: Computational parameters

Mesh size (no. elements)	200816
Time step size $[s]$	0.5
Extrusion time $[s]$	70
Heat treatment time $[s]$	70

Results

An overview of the microstructure obtained for a cross-section of the extrusion profile by LM images is given in Figure 4. The image is made of several small images stitched together to show the overall microstructure in the profile.

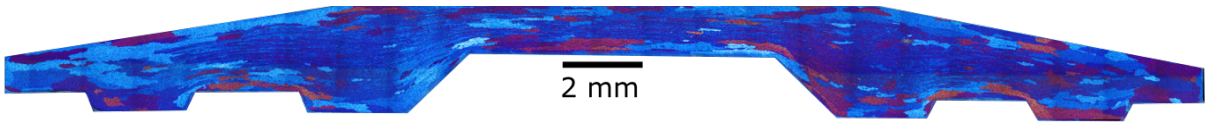

Fig. 4: Multiple images from Light Microscopy (LM) stitched together to give an impression of the whole microstructure.

Figure 5 shows a representation of the ruler profile with an overlay of several stitched EBSD maps after cooling on air preceding metal extrusion. It can clearly be seen how large grains are present near the surface while the inner part of the profile shows a rather fine microstructure.

Fig. 5: Multiple EBSD measurements stitched together to show the grain distribution for part of the ruler profile after metal extrusion.

In Figure 6, qualitatively similar results were obtained from numerical simulations. It can clearly be seen how large grains form near the profile surface, while grains in the inner part of the profile have a smaller size. The grain size is mainly influenced by the time between the profile exiting the die opening

and final cooling. The simulated results in Figure 6 were obtained after 70 s at constant temperature. A closer examination of the experimental procedure should help to tailor the thermal part (temperature, time, cooling rate) to quantitatively better fit the experimental results in the future. The distribution of

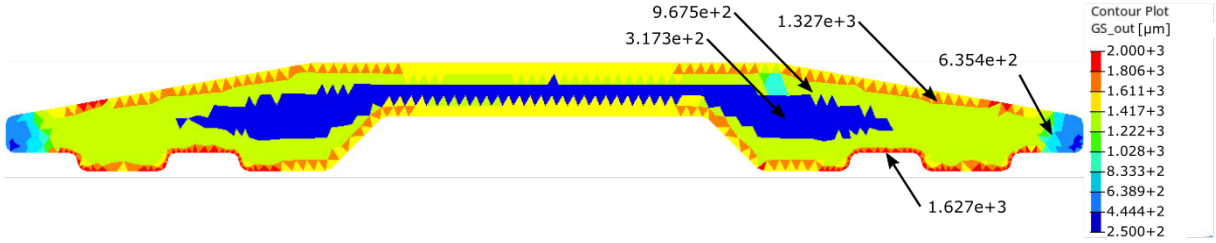

Fig. 6: Illustration of the grain size GS indicator on the profile cross-section after 70 s heat treatment.

potentially geometrically recrystallized areas are given in Figure 7. The gDRX indicator shows areas where grains can dynamically recrystallize. A comparison of Figure 6 and 7 show thus how grains grow to larger diameters in areas with GDRX = 1. It is determined during the forming simulation and triggered by Equation 8. Due to the coarse meshing, the individual elements are still visible in Figures

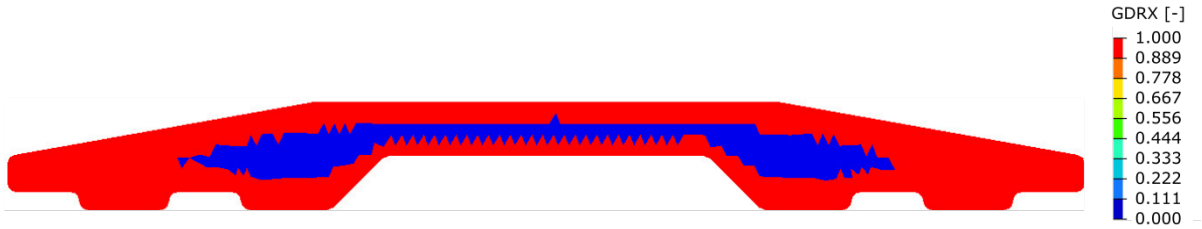

Fig. 7: Illustration of the gDRX indicator on the profile cross-section after 70 s heat treatment.

6 and 7. Finally, a usual way to verify the results from numerical extrusion simulations is a comparison of ram force which is given in Figure 8a. A reasonably good agreement between numerically predicted

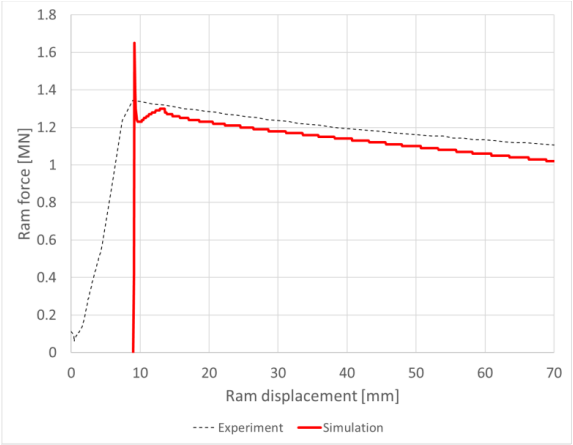

(a) Comparison of simulated ram force results with experiment.

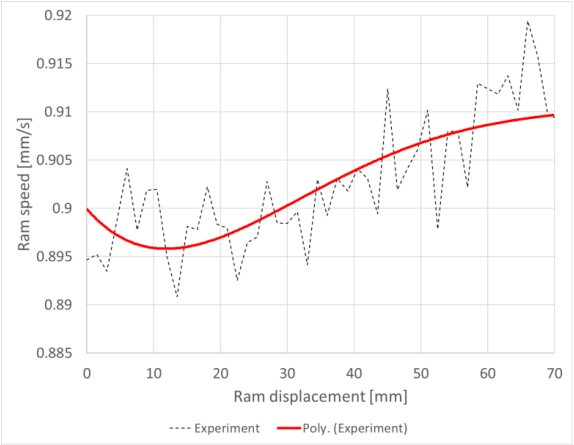

(b) Measured ram speed used in the simulation.

Fig. 8

and experimentally measured ram force could be achieved by considering the variation of ram speed (see Figure 8b) during the experiments in the simulation.

Conclusions

In present paper, the preliminary results from the implementation of a microstructure-based flow stress material model with subsequent grain growth simulation during a short heat-treatment phase is shown. The MD²M (Mean Dislocation Density Material) model was implemented as a user-defined function within the specialized metal extrusion simulation software HyperXtrude™. It was applied to simulate the production of a so-called ”ruler” profile with the aim to predict Peripheral Coarse Grain (PCG). Although those expectations could be fulfilled, several restrictions still apply:

- The material model is history based: Results need to be taken from time step to time step.
- Since there is generally no information about time, time step and nonlinear iteration available inside the UDF data array, a workaround was used by creating an artificial time.
- The use of such artificial time was only possible for fixed time step sizes and without nonlinear iterations.
- In the current implementation, heat treatment is simulated by reducing the ram speed to zero. This means that due to the restrictions in HyperXtrude™, the combined forming and heat-treatment time can only be the billet length divided by the ram speed.
- In the 2022 release of HyperXtrude™, a new functionality for simulating heat-treatment processes will be introduced which allows to separate the forming and the heat-treatment processes.

It is expected that further improvements in HyperXtrude™ by Altair will solve the open issues. The results given in this publications are also preliminary since it is necessary to improve the meshing, fine-tune the MD²M model and further investigate the influence of temperature and ram speed on the results of flow stress and grain growth models.

Acknowledgements

The authors would like to thank the Austrian Federal Ministry for Climate Action, Environment, Energy, Mobility, Innovation and Technology, Federal State of Upper Austria in the FD Framework (within PSHeRo:ER project OÖ Fin-010104/187) and also the Austrian Institute of Technology (AIT) for the technical/financial support in this research work. Special thanks to Dr. Andreas Schiffl and co-workers at Hammerer Aluminium Industries for supporting the work and insights into industrial metal extrusion industries.

References

[1] V. Očenášek, P. Sedláček: *The effect of surface recrystallized layers on properties of extrusions and forgings form high strength aluminium alloys*, 20. International Conference on Metallurgy and Materials, Brno, (2011)

[2] A. R. Eivani: *Simulation of peripheral coarse grain structure during hot extrusion of AA7020 aluminum alloy*, J. Manu. Proc. Vol. 57, (2020), pp. 881-892

[3] E. D. Sweet, S.K. Caraher, N. V. Danilova, X. Zhang: *Effects of extrusion parameters on coarse grain surface layer in 6xxx series extrusions*, In Proceedings of the Eighth International Aluminum Extrusion Technology Seminar, Vol. 1, (2004), pp. 115-126

[4] T. Shepard: *Extrusion of aluminium alloys*, Springer Science & Business Media, (2013)

[5] M. C. Poletti, M. Rodriguez-Hortalá, M. Hauser, C. Sommitsch: *Microstructure development in hot deformed AA6082*, Materials Science and Engineering A, Vol. 528, (2011), pp. 2423-2430

[6] W. H. van Geertruyden: *Formation of Recrystallization Textures after Hot Working of AA2014 and AA6063*, Material Science Forum. Vol. 408-412, (2002), pp. 845-850

[7] P. Sherstnev, A. Zamani: *Modelling of static and geometric dynamic recrystallization during hot extrusion of Al-Mg-Si alloy*, Material Science Forum. Vol. 794-796, (2014), pp. 728-733

[8] F. J. Humphreys, M. Harthely: *Recrystallization and related annealing phenomena*, 2nd ed., (2004)

[9] H. J. McQueen, E. Evangelista, M. E. Kassner: *The classification and determination of restoration mechanisms in the hot working of Al alloys*, Zeitschrift für Metallkunde, Vol. 82/5, (1991), pp. 336-345

[10] U. F. Kocks: *Laws for Work-Hardening and Low-Temperature Creep.*, ASME. J. Eng. Mater. Technol., Vol. 98(1), (1976), pp. 76-85, https://doi.org/10.1115/1.3443340

[11] H. Mecking, U. F. Kocks: *Kinetics of flow and strain-hardening*, Acta Metallurgica, Vol. 29, (1981), pp. 1865-1875

[12] T. Gladman: *On the theory of the effect of precipitate particles on grain growth in metals*, Proc. Roy. Soc. London, Vol. A294, (1966), pp. 298-309

[13] E. Nes, N.Ryum, O. Hunderi: *On the Zener drag*, Acta Metall, Vol. 33, (1985) pp. 11-22

[14] P. Sherstnev, C. Melzer, C. Sommitsch: *Prediction of precipitation kinetics during homogenisation and microstructure evolution during and after hot rolling of AA5083*, Int. J. Mech. Sci., Vol. 54, (2012), pp. 12-19

[15] J. A. Österreicher, et al. ”Information depth in backscattered electron microscopy of nanoparticles within a solid matrix.” Materials Characterization 138 (2018): 145-153.